

Detection and characterization of protein aggregates by fluorescence microscopy

Barthélemy Demeule, Robert Gurny, Tudor Arvinte*

Department of Pharmaceutics and Biopharmaceutics, School of Pharmaceutical Sciences, University of Geneva, University of Lausanne, 30 Quai Ernest-Ansermet, CH-1211 Geneva 4, Switzerland

Received 23 February 2006; received in revised form 11 August 2006; accepted 15 August 2006

Available online 26 August 2006

Abstract

Aggregation may compromise the stability as well as the biological activity of protein drugs. Detection of protein aggregates is needed in the process of protein characterization and during optimization of pharmaceutical formulations. This paper describes a technique, which consists of analysing protein aggregates by fluorescence microscopy after staining with the hydrophobic probe Nile Red. Dilution, filtration or other modifications of the sample are not needed. Assessment of aggregation was possible in highly concentrated protein samples (193 mg/ml). Fluorescence microscopy observations allowed the detection and characterization of protein aggregates not easily detected by spectroscopic techniques. Nile Red was shown to be very sensitive for the detection and analysis of immunoglobulin aggregates. Nile Red, Congo red and Thioflavine T stainings were compared. Nile Red and Thioflavine T fluorescence were colocalized. The diameter of immunoglobulin aggregates was determined, and the number of aggregates was correlated with 90° light scattering measurements. Studies of human calcitonin aggregates brought to light new aspects of the human calcitonin aggregation mechanisms. Thus, Nile Red staining not only allows detection of very low levels of protein aggregates, but also contributes to a better understanding of the complex mechanisms governing protein aggregation.

© 2006 Elsevier B.V. All rights reserved.

Keywords: Immunoglobulin; Calcitonin; Aggregation; Nile Red; Microscopy; Physical stability

1. Introduction

Protein drugs now constitute a significant proportion of the new molecular entities reaching the market (Walsh, 2005). Compared to most small molecular drugs, proteins are physico-chemically unstable and aggregation is one of the key elements compromising the protein's physical stability. Protein instability can appear early in development and may compromise the outcome of preliminary clinical trials. The problems caused by protein aggregation go beyond manufacturing and formulation. In the case of human calcitonin, aggregation was shown to reduce the efficacy of the drug (Cudd et al., 1995). Moreover, therapeutic protein aggregates can present a risk to the patient, since protein aggregates have been shown to be toxic in specific cases (Bucciantini et al., 2002). Aggregates formed by therapeutic proteins could also have toxic effects. Aggregates are one of the factors that can enhance the immunogenicity of

a protein drug (Hermeling et al., 2004), as shown in the case of interferon- α aggregates in mice (Braun et al., 1997).

Characterizing protein aggregation in a sample requires appropriate analytical methods. Several approaches should be combined to determine the sample aggregation, in order to overcome the limitations of a single method (Arvinte, 2005). The local environment of the protein is one factor influencing aggregation. Analytical methods often change the local environment of the protein, either by dilution or by contact with other substances such as eluents. An ideal method should be able to assess protein aggregation while minimizing changes in the local environment of the protein (Arvinte, 2005). Tools are needed for the study of proteins at high concentrations, especially in the case of formulations for subcutaneous administration (Shire et al., 2004). Size-exclusion chromatography is one of the methods most frequently used to characterize protein aggregates despite not meeting the above-mentioned requirements (Clodfelter et al., 1999).

In this paper, a fluorescence microscopy technique that complements existing analytical methods is described. The proposed method is based on the visualization and characterization of pro-

* Corresponding author. Tel.: +41 22 379 63 39; fax: +41 22 379 65 67.
E-mail address: tudor.arvinte@pharm.unige.ch (T. Arvinte).

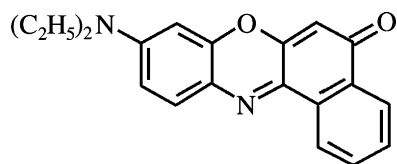


Fig. 1. Chemical structure of the hydrophobic dye Nile Red (9-diethylamino-5H-benzo[α]phenoxazine-5-one); m.w. 318.37.

tein aggregates after staining with the hydrophobic dye Nile Red. Nile Red is a low molecular weight phenoxazine dye (m.w. 318.37, Fig. 1) that has been well characterized (Davis and Hetzer, 1966; Greenspan and Fowler, 1985; Sackett and Wolff, 1987). Nile Red binds to hydrophobic surfaces of proteins. The hydrophobic surfaces of proteins are exposed, and therefore become available for Nile Red binding, during protein unfolding or in processes such as ligand–protein binding, protein oligomerization and fibril formation (Sackett and Wolff, 1987). In such a hydrophobic environment, Nile Red exhibits a strong fluorescence (high quantum yield) whereas in aqueous media Nile Red is relatively insoluble and its fluorescence is strongly quenched. The sensitivity of Nile Red to changes in its environment and its binding to protein surfaces have previously been exploited in the spectroscopic study of calcitonin fibrillation (Bauer et al., 1993). Using a fluorescence microscope, aggregates stained by Nile Red can be efficiently detected and characterized.

In medical research and pathology laboratories, two dyes are used in the detection of amyloids: Thioflavine T and Congo red (Westermarck et al., 1999; Nilsson, 2004). In the presence of amyloid deposits, Congo red exhibits an apple green birefringence and Thioflavine T fluorescence increases (Westermarck et al., 1999; Voropai et al., 2003; Nilsson, 2004). In the present study, Nile Red, Congo red and Thioflavine T staining of antibody aggregates were compared, and Nile Red was used to stain calcitonin fibrils. Nile Red was shown to be capable of binding to protein aggregates. Detection and characterization of aggregates by fluorescence microscopy was efficiently achieved even at high protein concentrations, minimizing changes in the protein local environment. Nile Red staining and the subsequent fluorescence microscopy analysis, together with Nile Red spectroscopy, can complement other staining techniques and analytical methods.

2. Materials and methods

2.1. Materials

Antibody A is an IgG1 recombinant humanized monoclonal antibody of about 150 kDa provided by Novartis Pharma AG, Basel, Switzerland. Antibody A was stored at 4 °C at a concentration of 193 mg/ml in a stock solution containing 0.1% acetic acid in 50 mM magnesium chloride. The solvent constitution of the stock solution ensures the chemical and physical stability of the antibody. All antibody solutions were prepared by dilution of this stock solution in the intended medium. Human calcitonin was provided by Novartis Pharma AG, Basel, Switzerland.

Nile Red (9-diethylamino-5H-benzo[α]phenoxazine-5-one) was purchased from Sigma (Buchs, Switzerland). Nile Red was dissolved in ethanol to produce a 100 μ M stock solution. Congo red and Thioflavine T were purchased from Fluka (Buchs, Switzerland). Congo red was dissolved in 80% ethanol and 20% water to produce a 720 μ M solution. Thioflavine T was dissolved in water at a concentration of 36 mM. Nile Red solution was stored at 4 °C, protected from light. Congo red and Thioflavine T solutions were prepared extemporaneously. All water used in the experiments was deionized by a Milli-Q academic system (Millipore, Billerica, USA). Antibody A and human calcitonin were stored at 4 °C. All experiments were performed at 25 °C.

2.2. Antibody concentration measurements

The concentration of antibody A solutions was determined by UV spectroscopy at 280 nm, based upon an absorbance of 1.6 for a 1 mg/ml solution in a 1-cm cell. The UV measurements were performed at 25 °C with a temperature-controlled Cintra 40 spectrophotometer (GBC, Melbourne, Australia). When the absorbance of an antibody solution at 400 nm was higher than the absorbance of the formulation buffer alone, the UV spectrum was corrected to account for the apparent absorbance due to light scattering (Drake, 1994). The UV spectrum of the solvent was subtracted from the UV spectrum of the antibody solution. The absorbance values were plotted as a function of wavelength (between 320 and 450 nm) according to the following equation:

$$\log(\text{absorbance}) = \text{slope} \times \log(\lambda) + \text{intercept}$$

The values of absorbance due to light scattering were extrapolated to the entire studied wavelength range and subtracted from the spectrum of the antibody solution (Drake, 1994).

2.3. Preparation of antibody aggregates

Antibody A aggregates were prepared by dilution of the stock solution (193 mg/ml) in 10 mM sodium phosphate buffer pH 7.0–7.2. Dilution factors ranged from 1:125 to 1:1000. The higher antibody concentrations produced a greater number of aggregates than the lower antibody concentrations. Antibody A concentrations were determined by UV spectroscopy, as mentioned above.

2.4. Staining techniques and microscopy

Staining was achieved with the addition of 0.5 μ l of the Nile Red, Congo red or Thioflavine T solution to 50 μ l of the protein solution. The exact experimental conditions for the protein solutions (pH, salt content) are described in each figure legend. Immediately after Nile Red addition, aliquots of the protein samples containing the dye were placed on Kova Glasstic slides (Hycor, Garden Grove, USA) and observed by microscopy. The observations were performed on an Axiovert 200 microscope (Zeiss, Göttingen, Germany) equipped with a mercury discharge lamp for fluorescence microscopy and a tungsten lamp for brightfield microscopy. A Zeiss filter cube no. 15 was used

for fluorescence microscopy with Nile Red (EX BP 546/12, BS FT 580, EM LP 590). A Zeiss filter cube no. 9 was used for fluorescence microscopy of Thioflavine T (EX BP 450–490, BS FT 510, EM LP 515). When Nile Red and Thioflavine T double-labelling was performed, a supplementary emission filter (BP 560/40) purchased from Chroma (Chroma Technology, Rockingham, USA) was added to the optical path of filter cube no. 9 to eliminate all Nile Red fluorescence. To visualize Congo red birefringence, crossed prism polarizers were added in the bright-field optical path. The images were acquired with a cooled Retiga 1300C colour CCD camera (QImaging, Burnaby, Canada) and processed using the Openlab version 3.1.7 software (Improvision, Coventry, UK). The observations were performed with 10 \times , 20 \times and 40 \times A-Plan LD objectives (Zeiss, Göttingen, Germany).

2.5. Particle counting

The samples, stained with Nile Red, were placed on Kova Glasstic slides (Hycor, Garden Grove, USA) and observed by fluorescence microscopy using a 10 \times objective. The Kova Glasstic slides display a square grid with a mesh size of 330 μ m. Particles were numbered in nine squares, representing a total volume of 0.1 μ l. The total number of particles was multiplied by 10 to obtain the number of particles per microliter.

2.6. Particle size

The samples, stained with Nile Red, were placed on Kova Glasstic slides (Hycor, Garden Grove, USA) and observed by fluorescence microscopy. Photomicrographs of several wells were taken using a 40 \times objective. In most cases, 100–300 particles were measured and the standard deviation of the diameter was calculated. In some cases, where few particles were present, only 30–70 particles could be measured. Image processing was performed with ImageJ version 1.29 (NIH, USA). The photomicrographs were calibrated and thresholded. The particles were analysed with the “Analyse Particles” function of the ImageJ software, which calculates the projected area of each individual particle. As the particles were spherical, the diameter of the particles was deduced from their projected area, excluding all particles smaller than the resolution limit of the microscope (1.5 μ m in diameter).

2.7. Fluorescence measurements

The fluorescence measurements were performed with a Fluoromax spectrofluorometer (Spex, Stanmore, UK) in a thermostatted cuvette holder. The Nile Red fluorescence was monitored between 580 and 750 nm, with an excitation wavelength of 560 nm. The spectra were recorded with a 0.01 s integration time per 1 nm increment. The excitation and emission slits were set to 1 and 3 mm, respectively. Nile Red fluorescence was measured at the wavelength of maximum emission, which ranged between 610 and 623 nm.

Nile Red and Thioflavine T excitation spectra were obtained for emission wavelengths of 630 and 495 nm, respectively. The

spectra were recorded with a 0.01 s integration time per 1 nm increment. The excitation and emission slits were set to 1 mm.

2.8. 90° light scattering

Light scattering intensity of protein solutions was measured with the Fluoromax spectrofluorometer (Spex, Stanmore, UK) between 350 and 750 nm, with the excitation and emission monochromators synchronized. The spectra were recorded with a 0.01 s integration time per 1 nm increment. The excitation slit was set to 1 mm. The emission slit was set to 0.5 or 1 mm. The aggregation state of the antibody in the samples was determined by monitoring light scattering intensity at 600 nm, or between 500 and 750 nm. The light scattering intensity is expressed as counts per second (cps).

2.9. Human calcitonin fibrillation

Freeze-dried human calcitonin was dissolved in 400 μ l of water. A volume of 0.1 M sodium acetate–acetic acid buffer pH 4.6 was added, resulting in a final solution of 7.3 mg/ml human calcitonin in 0.05 M sodium acetate buffer pH 4.6. The solution (800 μ l) was placed in an ultra-micro quartz fluorescence cell (Hellma, Müllheim, Germany) and 8 μ l of Nile Red solution were added (see Section 2.1). During the aggregation process, UV absorbance at 350 nm and Nile Red fluorescence were monitored at regular intervals. At each time point, two samples of 10 μ l each were taken and observed by Nile Red fluorescence microscopy.

3. Results

3.1. Staining and detection of antibody aggregates

Suspensions of antibody A aggregates in phosphate buffer (see Section 2.3) were divided into two parts. One part was visualized by brightfield microscopy and the other part was stained with Nile Red and visualized by fluorescence microscopy. A typical photomicrograph is displayed in Fig. 2. The aggregates are seen as black dots in the brightfield photomicrograph, and clear orange dots on a darker background in the fluorescence photomicrograph. Both protein solutions, with and without Nile Red, showed aggregates very similar in size, shape and number. Nile Red was added after the formation of aggregates in order to avoid interference with the antibody aggregation kinetics. The addition of Nile Red and the subsequent observation by fluorescence microscopy allowed a more efficient visualization of the protein aggregates compared to brightfield microscopy (Fig. 2). The advantage of staining and visualizing by Nile Red fluorescence microscopy was evident when few aggregates were present in the solutions. The higher contrast provided by fluorescence microscopy allowed the detection of aggregates present in small numbers, and the relative specificity of the Nile Red staining eliminated false positives due to small amounts of dust or impurities present in the buffer solution. Antibody A stock solution (193 mg/ml) did not exhibit visible aggregates when stained with Nile Red; dilution of the stock solution to 94 and 0.7 mg/ml

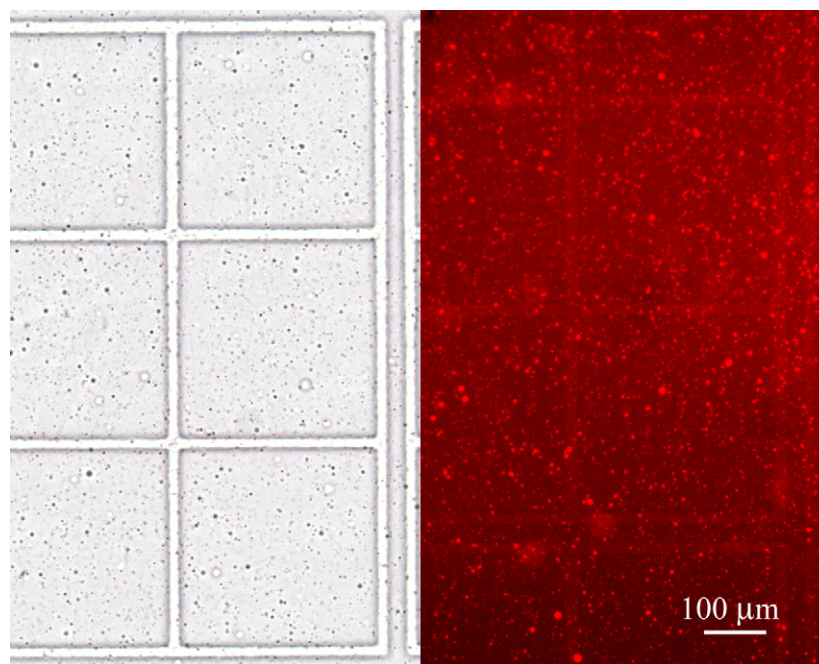


Fig. 2. (Left) Brightfield image of unstained antibody A aggregates in 10 mM phosphate buffer pH 7. (Right) Fluorescence image of the same antibody aggregates stained with Nile Red. Both methods showed aggregates similar in size and shape. Protein concentration was 0.8 mg/ml.

in 0.1% acetic acid containing 50 mM magnesium chloride did not induce aggregation (Fig. 3). The presence of 1 μ M Nile Red and 1% ethanol did not induce immediate aggregation nor did it modify the size or shape of the existing aggregates. The 90° light scattering measurements showed no differences in a solution before and after Nile Red addition (Fig. 4).

Photomicrographs taken the same day under the same conditions could reveal differences in the Nile Red fluorescence intensity between several solutions. Fig. 5 shows fluorescence spectra and fluorescence photomicrographs of antibody A solutions stained with Nile Red. At the same concentration of 0.71 mg/ml, Antibody A dissolved in acetic acid containing magnesium chloride exhibited a higher Nile Red fluorescence than when dissolved in 10 mM citrate buffer at the same pH. The difference in background fluorescence intensity is shown on the photomicrographs (Fig. 5). At equal concentrations and for a given protein, a higher Nile Red fluorescence indicates that more or different hydrophobic pockets are available for Nile Red binding, possibly in aggregates too small to be resolved by fluorescence microscopy, or reflecting changes in protein conformation.

3.2. Colocalization of Nile Red/Thioflavine T fluorescence and Congo red birefringence

Congo red and Thioflavine T are two dyes used for staining amyloid protein aggregates. Upon binding to amyloid fibrils such as β -amyloid, Congo red exhibits a characteristic apple-green birefringence when observed with crossed polarizers while Thioflavine T fluorescence is increased (Westermarck et al., 1999). Antibody A aggregates were not capable of binding Congo red: in the presence of antibody A aggregates, Congo red

did not exhibit any birefringence. However, antibody A aggregates were capable of binding Thioflavine T. Suspensions of antibody A aggregates in phosphate buffer were stained with both Nile Red and Thioflavine T (Fig. 6). Under the microscope, selection of appropriate filters allowed the separation of Nile Red fluorescence from Thioflavine T fluorescence. Nile Red and Thioflavine T fluorescence were entirely colocalized. Due to the Brownian motion of the smaller particles, separate green and orange dots were sometimes observed in the photomicrographs. In these dual staining experiments, the dye that was added first exhibited a stronger fluorescence than the dye that was added later.

3.3. Counting and sizing antibody aggregates

The 90° light scattering intensity is sensitive to the number and size of aggregates present in a solution. A correlation between particle number and the amount of scattered light was obtained in the case of antibody A aggregates (Fig. 7). Aggregation took place within seconds in the fluorescence cuvette when 10 μ l of Antibody A stock solution (193 mg/ml) were diluted in 2 ml sodium phosphate buffer, under 90° light scattering monitoring. A mild agitation was provided by a magnetic stirrer. After the onset of aggregation, the light scattering signal rapidly decreased following a very reproducible profile (data not shown). Sampling of the solution at five time points and examination by fluorescence microscopy allowed characterization of aggregates >1.5 μ m in diameter. Aggregate size remained constant during the experiment. The diameter of 62% of the aggregates was comprised between 2 and 4 μ m (Fig. 8). The decrease in the light scattering signal can be explained by a decrease in the number of aggregates, from 3500 to 1000 parti-

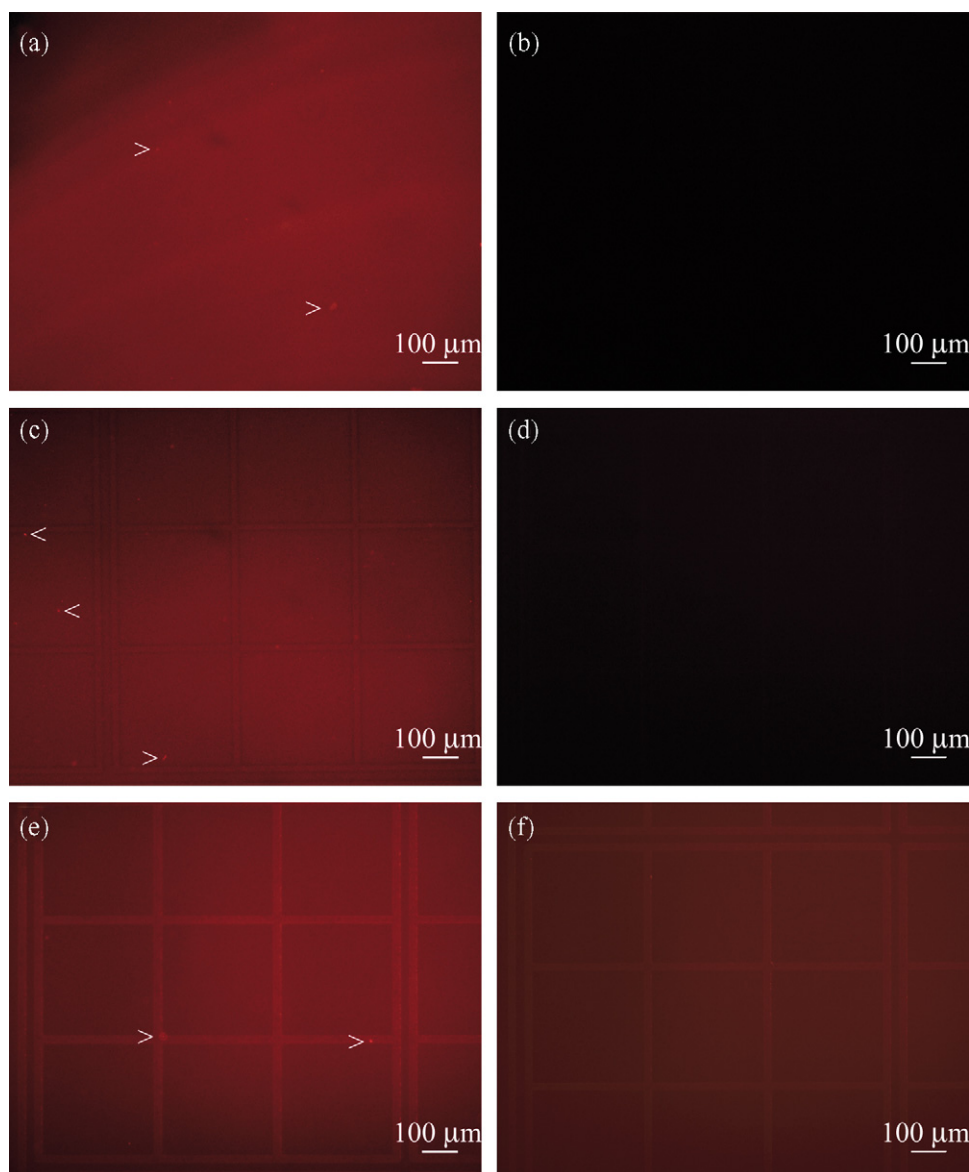


Fig. 3. Fluorescence microscopy of non-aggregated antibody A samples, formulated in 0.1% acetic acid containing 50 mM magnesium chloride, after staining with Nile Red (left). Photomicrographs of the formulation buffer alone taken under the same conditions are presented on the right side. (a) Antibody A stock solution (193 mg/ml), 280 ms exposure time. Very few dots can be noticed (arrows). The absence of gelation after several months storage indicates that the few particles observed were not the “seeds” leading to fibril formation but were probably dried protein material. (b) Formulation buffer stained with Nile Red, 280 ms exposure time. (c) Antibody A, 94 mg/ml, 600 ms exposure time. (d) Formulation buffer stained with Nile Red, 600 ms exposure time. (e) Antibody A, 0.7 mg/ml, 2 s exposure time. At a similar concentration, antibody A diluted in phosphate buffer exhibited strong aggregation (cf. Fig. 2). (f) Formulation buffer stained with Nile Red, 2 s exposure time.

cles per microliter over 7 h (Fig. 7). The decrease in the number of aggregates demonstrates the reversibility of antibody A aggregation in phosphate buffer.

3.4. Early detection of human calcitonin aggregation

In aqueous solutions, human calcitonin has a strong tendency to aggregate, resulting in a reduced potency (Cudd et al., 1995). Human calcitonin fibrillation kinetics have been previously studied by Nile Red fluorescence and UV absorption at 350 nm (Bauer et al., 1993). The experiment described by Bauer et al. (1993) was reproduced and samples were taken at regular

time intervals to be examined by fluorescence microscopy (Fig. 9). Accounting for small differences in calcitonin concentration, the fibrillation kinetics presented in Fig. 9 were identical to the results presented by Bauer et al., ending in the formation of a hard gel (Bauer et al., 1993). Aggregation kinetics show a lag-phase followed by a sigmoidal increase of the UV absorbance and Nile Red fluorescence signals. Nile Red fluorescence detected the aggregation phenomenon earlier than UV absorbance. However, fluorescence photomicrographs revealed that aggregates were present in the solution at the outset and increased in number and size with time. An increase in the number of aggregates was apparent during the lag-phase

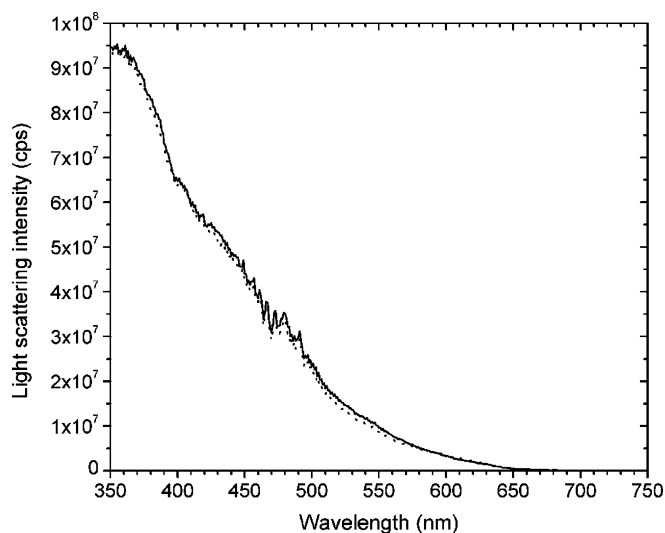


Fig. 4. The 90° light scattering spectra of antibody A in absence (solid line) and in presence (dotted line) of Nile Red. Antibody A was dissolved in 0.1% acetic acid containing 50 mM magnesium chloride. The addition of Nile Red did not increase the intensity of the light scattering signal. The aggregation state of the immunoglobulin was therefore not modified by the addition of Nile Red. Protein concentration was 80 mg/ml, comparable to the photomicrograph presented in Fig. 3c.

but was detected neither by UV absorbance nor by fluorescence intensity.

4. Discussion

Experiments performed with antibody A showed that Nile Red was a suitable dye for the study of protein aggregates by fluorescence microscopy. Nile Red is only weakly fluorescent in aqueous environments, but its fluorescence increases upon

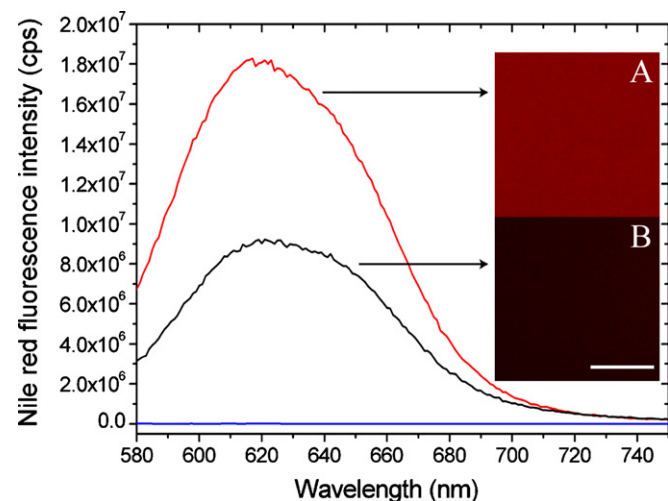


Fig. 5. Comparison of Nile Red fluorescence photomicrographs and Nile Red fluorescence spectra. Antibody A (0.71 mg/ml) was dissolved in 0.1% acetic acid containing 50 mM magnesium chloride (A) and in 10 mM citrate buffer pH 3.0 (B). Both photomicrographs were taken and processed the same day under the same conditions. The higher intensity of the Nile Red fluorescence in acetic acid containing magnesium chloride (red spectrum) corresponds to a more intense background in the photomicrograph (A). Scale bar is 100 μ m.

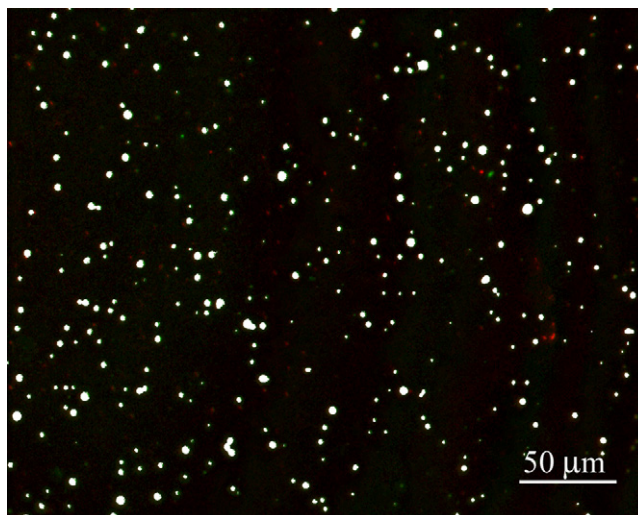


Fig. 6. Antibody A aggregates in 10 mM phosphate buffer pH 7 stained with both Nile Red (orange fluorescence) and Thioflavine T (green fluorescence). Colocalization of Nile Red and Thioflavine T fluorescence is represented in white. Nile Red and Thioflavine T fluorescence were entirely colocalized. (For interpretation of the references to colour in this figure legend, the reader is referred to the web version of the article.)

binding to the hydrophobic surfaces of proteins that are exposed during oligomerization (Sackett and Wolff, 1987). Typical Nile Red emission and excitation spectra are shown in Figs. 5 and 10. Protein aggregates may contain hydrophobic surfaces. Aggregates can bind Nile Red more efficiently than monomers and are easily detected by fluorescence microscopy. Solution properties such as buffer, salts, pH, and ionic strength define the protein formulation and have strong influences on the protein

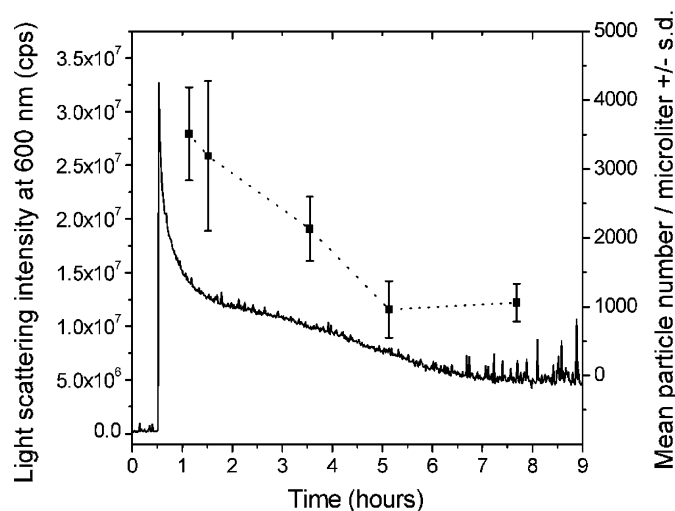


Fig. 7. Antibody A aggregation monitored during 9 h under mild agitation. The 90° light scattering signal (solid line) was acquired in the fluorometer. Initially, the cell was filled with 10 mM sodium phosphate buffer pH 7.16. After 30 min, 10 μ l of antibody A stock solution (193 mg/ml) were added. Aliquots were taken at four time points to be analysed by fluorescence microscopy after staining with Nile Red. The mean particle number was determined (squares; the bars indicate standard deviation). After a strong initial aggregation, the decrease in the light scattering signal was correlated with a decrease in the mean particle number. The particle size did not change during the experiment.

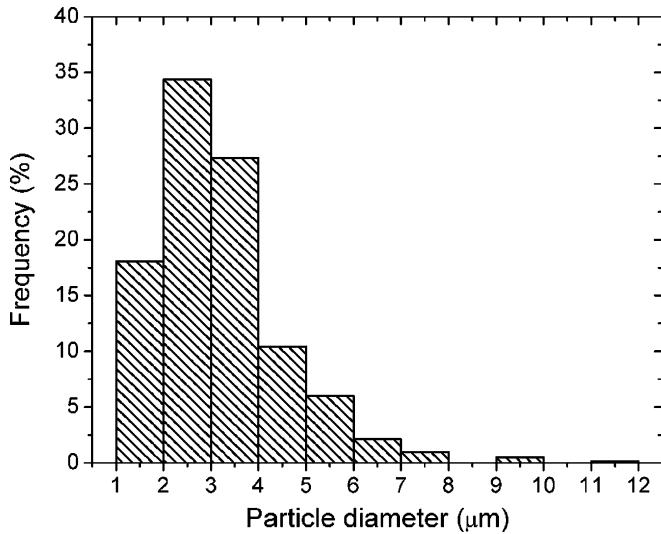


Fig. 8. Size distribution of antibody A aggregates in 10 mM phosphate buffer pH 7. Particle size was evaluated by fluorescence microscopy after staining with Nile Red. The diameter of 62% of the particles was comprised between 2 and 4 μm (mean: 3.18 μm), $n = 614$.

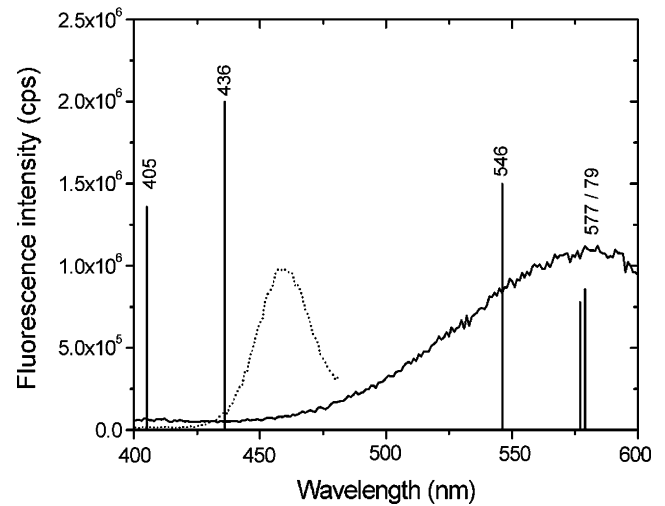


Fig. 10. Nile Red (solid line) and Thioflavine T (dotted line) fluorescence excitation spectra. Typical spectral lines from a mercury discharge lamp are displayed. Excitation spectra allow determining at which wavelength a fluorophore is efficiently excited. Under the microscope, Nile Red molecules can be excited by the 546 nm mercury discharge line (typically with filter cubes used for rhodamine B) whereas Thioflavine T can only be weakly excited by mercury lamps.

aggregation. In aqueous environments Nile Red fluorescence is not affected by solution properties and changes in Nile Red fluorescence reflect mainly changes in protein conformation or aggregation. The Nile Red fluorescence microscopy method described in the present paper allows the detection and charac-

terization of protein aggregates in a very broad size range from 0.5 μm to millimetres. Characterization of particles >0.5 μm in size is of interest because many analytical methods require sample preparation steps such as filtration that prevent the detection of large particles. Nile Red fluorescence microscopy allows the

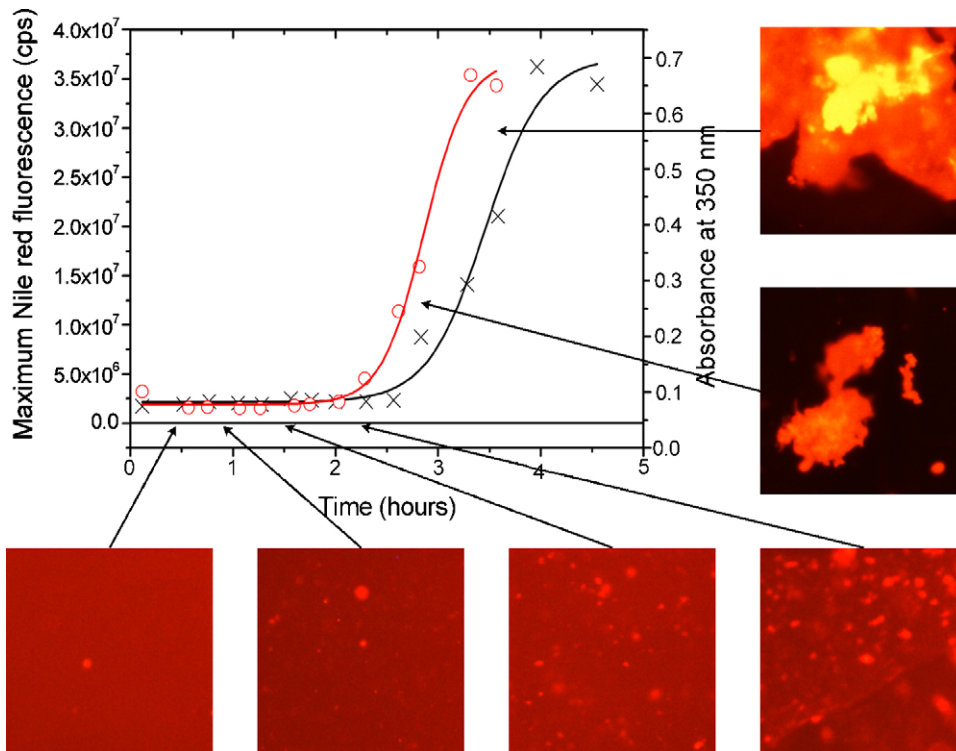


Fig. 9. Human calcitonin fibrillation in 0.05 M acetate buffer pH 4.6 followed by microscopy, Nile Red fluorescence and UV absorbance at 350 nm. All the data were obtained from the same solution. Nile Red fluorescence (○) detected the gelation phenomenon earlier than UV absorbance (×). Only the microscopic study of the Nile Red-stained solutions revealed that aggregates were present in the solution from the beginning and increased in number with time even in the “lag-phase”. The solution finally became a turbid gel. The photomicrograph dimensions are 301 μm × 301 μm. The contrast of the first four photomicrographs was enhanced to allow visualization of the aggregates.

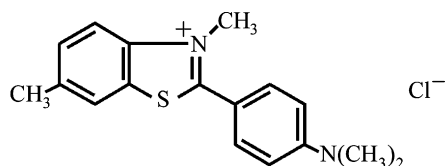


Fig. 11. Chemical structure of Thioflavine T (2-[*p*-(dimethylamino)phenyl]-3,6-dimethylbenzothiazolium chloride); m.w. 318.87.

characterization of turbid and concentrated protein solutions, as in vaccines or subcutaneous injections, respectively. Nile Red fluorescence microscopy is one of the few methods allowing aggregates characterization *in situ*, in presence of excipients. The ability to detect few large aggregates in a wide range of experimental conditions is particularly relevant to the field of pharmaceutical sciences.

Human calcitonin fibrillation is a well characterized phenomenon (Bauer et al., 1993, 1995; Arvinte et al., 1993; Cudd et al., 1995). Nile Red fluorescence microscopy permitted the detection of aggregates in the solution during the fibrillation lag-phase (Fig. 9). The early aggregates were not detected by UV absorbance or fluorescence spectroscopy but could be visualized by fluorescence microscopy after staining with Nile Red. We propose that the early aggregates represent “seeds” leading to further fibril formation and observed gelation: with time, the human calcitonin aggregates grew in number and formed larger structures. Spectroscopic methods failed in the detection of the “seeds” because they represent a small proportion of the protein molecules and have no impact on the *average* properties of the solution. Thus, the contrast enhancement obtained by Nile Red staining provided a valuable tool for the early detection of small numbers of aggregates present in protein solutions.

Thioflavine T, a dye used for the detection of amyloid in tissues (Westermarck et al., 1999), stained antibody A aggregates. Nile Red and Thioflavine T fluorescence were colocalized (Fig. 6). In double labelling experiments, the dye that was applied first to the aggregates exhibited a stronger fluorescence, indicating that Thioflavine T and Nile Red may compete for binding to the *same* site on the protein aggregates. The structurally different dyes Thioflavine T (Fig. 11) and Nile Red (Fig. 1) have shown relatively non-specific binding to proteins (Sackett and Wolff, 1987; Westermarck et al., 1999). The lack of specificity could explain why these different dyes were able to stain the same aggregates. The positively charged Thioflavine T, being water soluble, has an advantage over Nile Red in that it eliminates the need to introduce ethanol in the samples. However, a higher quantity of Thioflavine T had to be used in order to obtain a fluorescence comparable in intensity to Nile Red; Thioflavine T was used at a concentration of 360 μM whereas Nile Red was used at a concentration of 1 μM . Fluorescence excitation spectra of Thioflavine T showed how a good excitation for Thioflavine T would be in a wavelength range that is far from mercury spectral lines (Fig. 10). The fluorescence intensity of Thioflavine T was therefore low under the microscope. As most fluorescence microscopes are equipped with mercury discharge lamps for sample illumination, Nile Red provides a brighter stain, since it can be excited by the 546 nm mercury spectral line.

The affinity of antibody A aggregates for Thioflavine T raised the question of the nature of the aggregates. Thioflavine T is reported to bind to amyloid plaques, which present a fibrillar structure (Voropai et al., 2003). Antibody A aggregates were not able to bind to Congo red, another dye used in the diagnostic of amyloidosis (Westermarck et al., 1999; Jin et al., 2003; Sen and Basdemir, 2003; Giorgadze et al., 2004). Antibody A aggregation was shown to be reversible (Fig. 7), and the size and shape of the aggregates were not similar to previously described immunoglobulin fibrils (Helms and Wetzel, 1996). The shape of the aggregates and the reversibility of aggregation indicate that antibody A aggregates in phosphate buffer are likely to be amorphous. Congo red has been considered more specific to amyloid fibrils than other dyes; however, its binding to native, partially folded proteins has indicated that binding specificity was poorer than anticipated (Khurana et al., 2001). Given the strict requirements of the staining procedures, amyloid fibrils can be overlooked in a Congo red assay (Westermarck et al., 1999). Literature indicates that interpreting photomicrographs of stained samples should be performed with care. The lack of specificity for amyloid fibrils can be an advantage when using Nile Red and Thioflavine T for the detection of protein aggregates in amorphous aggregates. Work performed in our laboratory showed that in some cases Nile Red did not stain all types of protein aggregates, underlining the need to use several dyes and analytical methods to assess protein aggregation.

Fluorescence microscopy after staining with Nile Red allows an early detection of changes in protein solutions, while minimizing alterations to the observed sample. In protein formulation, the ability to detect aggregates with Nile Red at early time points can accelerate stability testing and reduce the number of samples in long-term stability studies. Fluorescence microscopy provides the possibility of studying subtle changes in the aggregation state of proteins, which is also of interest in medicine and biology, whenever protein characterization is needed. Fluorescence microscopy allows the characterization of high-concentration protein formulations without dilution and with minimal impact on the protein's local environment.

Acknowledgement

We thank Novartis Pharma AG for providing antibody A and human calcitonin.

References

- Arvinte, T., 2005. Analytical methods for protein formulations. In: Jiskoot, W., Crommelin, D.J. (Eds.), *Methods for Structural Analysis of Protein Pharmaceuticals*. AAPS Press, Arlington, VA, pp. 661–666.
- Arvinte, T., Cudd, A., Drake, A.F., 1993. Studies of human calcitonin secondary structure and of the fibrillation phenomena. In: Schneider, C.H., Eberle, A.N. (Eds.), *Peptides 1992. Proceedings of the 22nd European Peptide Symposium*. ESCOM Science Publishers B.V., Leiden, The Netherlands, pp. 503–504.
- Bauer, H.H., Aebi, U., Haner, M., Hermann, R., Muller, M., Merkle, H.P., 1995. Architecture and polymorphism of fibrillar supramolecular assemblies produced by *in vitro* aggregation of human calcitonin. *J. Struct. Biol.* 115, 1–15.
- Bauer, H.H., Drake, A.F., Merkle, H.P., Arvinte, T., 1993. Fluorescence study of human calcitonin fibrillation kinetics using the hydrophobic probe Nile

- red. In: Schneider, C.H., Eberle, A.N. (Eds.), *Peptides 1992. Proceedings of the 22nd European Peptide Symposium*. ESCOM Science Publishers B.V., Leiden, The Netherlands, pp. 505–506.
- Braun, A., Kwee, L., Labow, M.A., Alsenz, J., 1997. Protein aggregates seem to play a key role among the parameters influencing the antigenicity of interferon alpha (IFN-alpha) in normal and transgenic mice. *Pharm. Res.* 14, 1472–1478.
- Bucciantini, M., Giannoni, E., Chiti, F., Baroni, F., Formigli, L., Zurdo, J., Taddei, N., Ramponi, G., Dobson, C.M., Stefani, M., 2002. Inherent toxicity of aggregates implies a common mechanism for protein misfolding diseases. *Nature* 416, 507–511.
- Clodfelter, D.K., Nussbaum, M.A., Reilly, J., 1999. Comparison of free solution capillary electrophoresis and size exclusion chromatography for quantitating non-covalent aggregation of an acylated peptide. *J. Pharm. Biomed. Anal.* 19, 763–775.
- Cudd, A., Arvinte, T., Das, R.E., Chinni, C., MacIntyre, I., 1995. Enhanced potency of human calcitonin when fibrillation is avoided. *J. Pharm. Sci.* 84, 717–719.
- Davis, M.M., Hetzer, H.B., 1966. Titrimetric and equilibrium studies using indicators related to Nile Blue A. *Anal. Chem.* 38, 451–461.
- Drake, A.F., 1994. The measurement of electronic absorption spectra in the ultraviolet and visible. In: Jones, C., Mulloy, B., Thomas, A.H. (Eds.), *Methods in Molecular Biology. Microscopy, Optical Spectroscopy and Macroscopic Techniques*, vol. 22. Humana Press Inc., Totowa, NJ, pp. 173–182.
- Giorgadze, T.A., Shiina, N., Baloch, Z.W., Tomaszewski, J.E., Gupta, P.K., 2004. Improved detection of amyloid in fat pad aspiration: an evaluation of Congo red stain by fluorescent microscopy. *Diagn. Cytopathol.* 31, 300–306.
- Greenspan, P., Fowler, S.D., 1985. Spectrofluorometric studies of the lipid probe, Nile red. *J. Lipid Res.* 26, 781–789.
- Helms, L.R., Wetzel, R., 1996. Specificity of abnormal assembly in immunoglobulin light chain deposition disease and amyloidosis. *J. Mol. Biol.* 257, 77–86.
- Hermeling, S., Crommelin, D.J., Schellekens, H., Jiskoot, W., 2004. Structure-immunogenicity relationships of therapeutic proteins. *Pharm. Res.* 21, 897–903.
- Jin, L.W., Claborn, K.A., Kurimoto, M., Geday, M.A., Maezawa, I., Sohraby, F., Estrada, M., Kaminsky, W., Kahr, B., 2003. Imaging linear birefringence and dichroism in cerebral amyloid pathologies. *Proc. Natl. Acad. Sci. USA* 100, 15294–15298.
- Khurana, R., Uversky, V.N., Nielsen, L., Fink, A.L., 2001. Is Congo red an amyloid-specific dye? *J. Biol. Chem.* 276, 22715–22721.
- Nilsson, M.R., 2004. Techniques to study amyloid fibril formation in vitro. *Methods* 34, 151–160.
- Sackett, D.L., Wolff, J., 1987. Nile red as a polarity-sensitive fluorescent probe of hydrophobic protein surfaces. *Anal. Biochem.* 167, 228–234.
- Sen, S., Basdemir, G., 2003. Diagnosis of renal amyloidosis using Congo red fluorescence. *Pathol. Int.* 53, 534–538.
- Shire, S.J., Shahrokh, Z., Liu, J., 2004. Challenges in the development of high protein concentration formulations. *J. Pharm. Sci.* 93, 1390–1402.
- Voropai, E.S., Samtsov, M.P., Kaplevskii, K.N., Maskevich, A.A., Stepuro, V.I., Povarova, O.I., Kuznetsova, I.M., Turoverov, K.K., Fink, A.L., Uverskii, V.N., 2003. Spectral properties of Thioflavin T and its complexes with amyloid fibrils. *J. Appl. Spectrosc. (Translation of Zhurnal Prikladnoi Spektroskopii)* 70, 868–874.
- Walsh, G., 2005. Biopharmaceuticals: recent approvals and likely directions. *Trends Biotechnol.* 23, 553–558.
- Westermarck, G.T., Johnson, K.H., Westermarck, P., 1999. Staining methods for identification of amyloid in tissue. *Meth. Enzymol.* 309, 3–25.